JOURNAL OF THERMOPHYSICS AND HEAT TRANSFER
Vol. 25, No. 1, January–March 2011

Numerical Inverse Heat Transfer Analysis for Temperature-Sensitive-Paint Measurements in Hypersonic Tunnels

Zemin Cai*
Shantou University, 515063 Shantou, People's Republic of China
Tianshu Liu† and Bo Wang‡
Western Michigan University, Kalamazoo, Michigan 49008
and
Justin Rubal§ and John P. Sullivan¶
Purdue University, West Lafayette, Indiana 47907

DOI: 10.2514/1.49217

This paper describes a numerical inverse method used in temperature-sensitive-paint measurements for quantitative global heat flux diagnostics in hypersonic tunnels. An iterative algorithm is developed to solve the one-dimensional inverse heat transfer problem for unsteady heat flux into a polymer layer (temperature-sensitive paint) on a semi-infinite base, where the temperature dependencies of the thermal properties of materials are taken into account. Surface heat flux distributions on cone models are calculated by using this algorithm from temperature-sensitive-paint images acquired in hypersonic wind tunnel testing.

Nomenclature

a	=	thermal diffusivity
c	=	specific heat
I	=	luminescent intensity
k	=	thermal conductivity
L	=	polymer thickness
q_s	=	surface heat flux
$q_{s(1D)}$	=	surface heat flux obtained by using the one-dimensional method
T	=	temperature
T_{in}	=	initial temperature
t	=	time
x, z	=	coordinates on surface
y	=	coordinate in normal direction to surface
ε	=	$\sqrt{k_p\rho_p c_p/k_b\rho_b c_b}$
θ	=	temperature change from initial temperature
θ_{ps}	=	temperature change on polymer surface
ρ	=	density

Subscripts

b	=	base
in	=	initial
p	=	polymer
ps	=	polymer surface
s	=	surface

Received 4 February 2010; revision received 9 July 2010; accepted for publication 2 October 2010.

*Associate Professor, Department of Electronic Engineering.
†Professor, Department of Mechanical and Aeronautical Engineering, G-220, Parkview Campus; tianshu.liu@wmich.edu. Senior Member AIAA (Corresponding Author).
‡Visiting Scientist, leave from Academy of Mathematics and Systems Science, Chinese Academy of Sciences, 100190 Beijing, People's Republic of China.
§Graduate Research Assistant, School of Aeronautics and Astronautics.
¶Professor, School of Aeronautics and Astronautics.

I. Introduction

TEMPERATURE-SENSITIVE paint (TSP) is able to provide quantitative global heat transfer diagnostics on hypersonic vehicles which is critical for the design of air vehicles [1–7]. The main problem in TSP measurements in hypersonic tunnels is how to accurately extract heat flux fields on a model surface from a time sequence of surface temperature fields. This is often considered as an inverse heat transfer problem. The transient solutions of the one-dimensional time-dependent heat conduction equation has been used in heat flux calculations from in aerothermodynamic measurements hypersonic wind tunnels [8]. The Cook–Felderman method based on the classical one-dimensional transient solution for a semi-infinite body has been widely used to calculate heat flux from a time history of surface temperature [9]. This one-dimensional method has been further adapted to process thermographic phosphor data obtained on a model injected to a hypersonic wind tunnel [10,11]. The performance of several one-dimensional methods has been evaluated by Walker and Scott [12]. The three-dimensional inverse heat transfer method has been used in thermochromic liquid crystal measurements to determine the surface heat transfer coefficient distributions [13,14]. In aerothermodynamic measurements, however, a temperature-sensitive coating like TSP as a polymer layer usually alters a history of the surface temperature, and therefore the effect of the coating itself on heat flux calculation should be taken into account.

Recently, Liu et al. [15] have given a one-dimensional analytical inverse solution for calculating heat flux from TSP surface temperature measurements (including other temperature-sensitive coatings). Here, the solution is briefly recapitulated for convenience of reading. Figure 1 shows a thin polymer layer on a semi-infinite base and a coordinate system used in this study. The transient solution of the one-dimensional time-dependent heat conduction equation is sought by inverting the Laplace transform for a thin polymer on a semi-infinite base. The heat flux given by the one-dimensional solution at the polymer surface is

$$q_{s(1D)}(t) = \frac{k_p(1-\bar{\varepsilon}^2)}{\sqrt{\pi a_p}} \int_0^t \frac{\bar{W}(t-\tau,\bar{\varepsilon})}{\sqrt{t-\tau}} \frac{\mathrm{d}\theta_{ps}(\tau)}{\mathrm{d}\tau}\,\mathrm{d}\tau \tag{1}$$

where $\theta_{ps}(t) = T(t,L) - T_{in}$ is the temperature change at the polymer surface from the initial temperature T_{in}, L is the polymer layer thickness, and a modified Gaussian integral for the effect of the polymer layer is

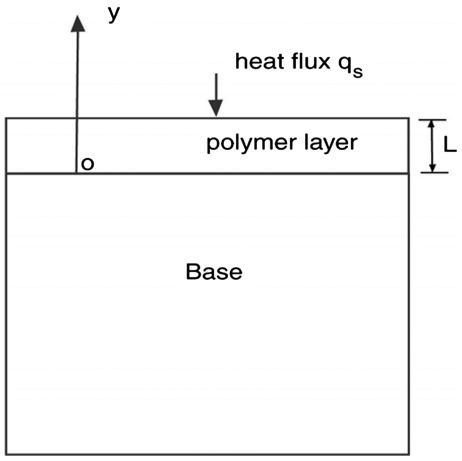

Fig. 1 A polymer layer on a semi-infinite base.

$$\bar{W}(t,\bar{\varepsilon}) = \frac{2}{\sqrt{\pi}}\int_0^\infty \frac{\exp(-\xi^2)\,\mathrm{d}\xi}{1+\bar{\varepsilon}^2 - 2\bar{\varepsilon}\cos(2L\xi/\sqrt{a_p t})} \tag{2}$$

The parameter $\bar{\varepsilon}$ is defined as $\bar{\varepsilon} = (1-\varepsilon)/(1+\varepsilon)$, where $\varepsilon = \sqrt{k_p\rho_p c_p / k_b\rho_b c_b}$, k_p, c_p and ρ_p are the thermal conductivity, specific heat and density of the polymer, respectively, k_b, c_b and ρ_b are the thermal conductivity, specific heat and density of the base material, respectively, and $a_p = k_p/c_p\rho_p$ is the thermal diffusivity of the polymer. For $\bar{\varepsilon} = 0$, Eq. (1) recovers the classical solution for a semi-infinite base since $\bar{W}(t,0) = 1$. This means that the function $\bar{W}(t,\bar{\varepsilon})$ represents the effect of the polymer layer (or TSP itself) on the determination of heat flux, which depends on $\bar{\varepsilon}$, a_p and L. The discrete form of Eq. (1) for actual calculation of heat flux can be considered as a generalization of the Cook–Felderman method for a combination of a polymer layer and a semi-infinite base of any material.

Generally, Eq. (1) is able to give reasonable results when it is applied to a three-dimensional model in tests in a short-duration wind tunnel. However, in a general three-dimensional case, heat conduction in the lateral direction may be significant in certain locations where the spatial gradient in heat flux is large. This situation occurs near shocks, shock/shock interaction, shock/boundary-layer interaction, boundary-layer transition, flow separation, and strong vortex/wall interaction. Further improvement should be made by correcting the lateral heat conduction effect. According to Liu et al. [16], the heat flux field $q_{s(1\mathrm{D})}(t,x,z)$ obtained by using the one-dimensional inverse method (either the analytical or numerical method) on a surface in a general three-dimensional case is related the true heat flux $q_s(t,x,z)$ in the three-dimensional case by the following equation:

$$q_{s(1\mathrm{D})}(t,x,z) = \int_{-\infty}^{\infty}\int_{-\infty}^{\infty} g(\sigma_r(t), x-x', z-z')q_s(t,x',z')\,\mathrm{d}x'\,\mathrm{d}z' \tag{3}$$

The filter in Eq. (3) is the Gaussian distribution:

$$g(t,x,z) = \frac{1}{2\pi\sigma_r^2(t)}\exp\left(-\frac{x^2+z^2}{2\sigma_r^2(t)}\right) \tag{4}$$

where $\sigma_r(t)$ is an empirical standard deviation that represents the effect of the lateral heat conduction, and t is the time elapsing from the start-up of a wind tunnel. According to Eq. (3), due to the lateral heat conduction effect, $q_{s(1\mathrm{D})}(t,x,z)$ is a blurred (filtered or diffused) representation of a true heat flux field $q_s(t,x,z)$. Equation (3) can be used as an approximate model for correcting the lateral heat conduction effect as long as $\sigma_r(t)$ is appropriately modeled. Given $q_{s(1\mathrm{D})}(t,x,z)$, $q_s(t,x,z)$ can be recovered by solving the convolution-type integral equation Eq. (3) as an image deconvolution problem [16]. Although a three-dimensional inverse heat conduction problem could be solved [13,14], the aforementioned alternative is a two-step method that is a combination of the one-dimensional inverse method and the two-dimensional (image) deconvolution method based on an analogy between the one-dimensional and three-dimensional solutions of the heat conduction equation.

Most analytical methods are based on an assumption that the thermal properties (thermal conductivity, specific heat and density) of a TSP (a polymer layer) are independent of temperature. In fact, the thermal properties are sensitive to temperature [17]. When a change of surface temperature is significantly large in high-enthalpy hypersonic tunnels, the assumption of constant thermal properties may produce a considerable error in heat flux calculation if the temperature effects on the thermal properties are not taken into account. In this case, since no exact analytical solution can be obtained, a numerical inverse method has to be sought.

The objective of this work is to present a numerical development parallel to the analytical inverse analysis given by Liu et al. [15] to calculate heat flux from TSP measurements. In TSP measurements, a white insulating layer (a thermally resistant base coating) is usually used for enhancing the luminescent light from TSP detected by a camera. In addition, this layer with a suitable thickness can be used to control the magnitude of the surface temperature change during a test. In this analysis, since both a TSP layer and an insulating layer are polymers with similar thermal properties, a combination of a TSP layer and an insulating layer is treated as a single polymer layer. Therefore, a polymer layer with a thickness on a semi-infinite substrate (in practice a sufficient thick base with 100 thermal diffusion length scales) is studied. The first step is to solve the direct heat transfer problem for the two-layer system, which is required not only for simulations but also for the development of the numerical inverse heat flux estimation algorithm. The inverse heat transfer method starts from initial determination of heat flux by using a simple and fast approximation calculation. As the second step, an iterative algorithm refines the estimation through optimization. The inverse heat transfer algorithm is examined through simulations. Given a simulated heat transfer history and the temperature-dependent thermal properties, the surface temperature change on a polymer layer on a semi-infinite base (aluminum and Nylon-6) is obtained accurately by numerically solving the heat conduction equation (the direct heat transfer problem). Then, from the surface temperature change, the inverse heat transfer algorithm is used to recover heat flux for a direct comparison with the known heat flux history and the result given by the analytical inverse method. Applications of the numerical inverse heat transfer method in TSP measurements in hypersonic wind tunnels are described.

II. Finite Difference Method for Direct Heat Transfer Problem

Figure 1 shows a polymer layer with a thickness L on a semi-infinite base and the coordinate system. There are two regions in our problem: polymer layer and semi-infinite base. In the direct problem, the heat flux $q_s(t)$ into the polymer surface is known as a function of time t. We want to obtain the distribution of the temperature change $\theta(y,t) = T - T_{\mathrm{in}}$ in the polymer and base by numerically solving the one-dimensional time-dependent heat conduction equation. For the polymer layer, the heat conduction equation is

$$\left(\frac{\partial}{\partial t} - a_p\frac{\partial^2}{\partial y^2}\right)\theta_p(y,t) = 0 \tag{5}$$

where $\theta_p(y,t) = T_p - T_{\mathrm{in}}$ is the temperature change of the polymer layer from a constant initial temperature T_{in}, and $a_p = k_p/c_p\rho_p$ is the thermal diffusivity of the polymer in which k_p, c_p and ρ_p are the thermal conductivity, specific heat and density of the polymer, respectively. The boundary condition at the polymer surface ($y = L$) is $q_s - k_p\partial\theta_p/\partial y = 0$, where $q_s(t)$ is the heat flux into the polymer surface and L is the polymer layer thickness. The origin of coordinates is set at the interface between polymer layer and base, as shown in Fig. 1. The initial condition for the polymer layer is $\theta_p(y,0) = 0$.

Table 1 Iterative algorithm

Input: measured surface temperature $\theta_{\mathbf{ps}}$ (TSP data)
Initialization:
1) Initialize error tolerance ε and construct matrix Φ
2) Compute coarse determination of heat flux q_{s_1} using $\theta_{\mathrm{ps}} = \Phi q_s$
3) From the direct heat conduction equations, compute θ'_{ps_1}
4) Calculate the temperature error $T_{\mathrm{err}} = \|\theta_{\mathrm{ps}} - \theta'_{\mathrm{ps}_1}\|_2^2$
5) $k = 1$
While $T_{\mathbf{err}} > \varepsilon$, repeat
Step 1. From the matrix form $\Phi q_{\mathrm{err}} = T_{\mathrm{err}}$, compute q_{err}
Step 2. $q_{s_{k+1}} = q_{s_k} + q_{\mathrm{err}}$
Step 3. Compute surface temperature $\theta'_{\mathrm{ps}_{k+1}}$ using the direct heat conduction equations
Step 4. Update $T_{\mathrm{err}} = \|\theta_{\mathrm{ps}} - \theta'_{\mathrm{ps}_{k+1}}\|_2^2$
Step 5. $k = k + 1$
End
Output: heat flux estimate $q_{s_{k-1}}$

Similarly, the equation for the base is

$$\left(\frac{\partial}{\partial t} - a_b \frac{\partial^2}{\partial y^2}\right)\theta_b(y,t) = 0 \tag{6}$$

where $\theta_b(y,t) = T_b - T_{\mathrm{in}}$ is the temperature change of the base layer from a constant initial temperature, and $a_b = k_b/c_b\rho_b$ is the thermal diffusivity of the base. The initial condition for the base is $\theta_b(y,0) = 0$. The boundary condition at infinity in the base is $\theta_b(-\infty,t) = 0$. The matching conditions at the interface between the two layers ($y = 0$) are $\theta_p = \theta_b$ and $k_p\partial\theta_p/\partial y = k_b\partial\theta_b/\partial y$.

Combination of the preceding equations and the boundary conditions gives a system of the two-region heat conduction equations with the known initial and boundary conditions. Here the direct (forward) heat conduction problem is to find the temperature fields $\theta_p(y,t)$ and $\theta_b(y,t)$ by using the standard finite difference method. Finite difference solution of the general heat conduction equation is discussed by Morton and Mayers [18], Fletcher [19] and Hoffman [20].

III. Inverse Algorithm for Determination of Heat Flux from TSP Data

Given a history of the polymer surface temperature θ_{ps} obtained from TSP measurements, the surface heat flux q_s is computed. This is an inverse heat transfer problem for the system of equations. Some methods for the conventional inverse heat conduction problem have been previously developed, such as sequential function specification methods and regularization methods [21–23]. In this paper, an iterative algorithm is proposed to solve this two-region inverse heat conduction problem. The initial step is based on the direct numerical method introduced in the preceding section, which is called initial determination of surface heat flux.

A. Initial Determination

For initial estimation, a linear matrix equation relating the surface heat flux and surface temperature data is proposed, i.e., $\theta_{\mathrm{ps}} = \Phi q_s$, where θ_{ps} and q_s denote a measured polymer surface temperature vector and a surface heat flux vector, respectively, and Φ is the relation matrix. If Φ is defined and nonsingular, then $q_s = \Phi^{-1}\theta_{\mathrm{ps}}$. However, the actual functional relation between the temperature data θ_{ps} and heat flux q_s is complicated, which is related to the thermal properties of the polymer and base layers. As an initial step of the iterative algorithm, we try to find the approximate relation matrix Φ' based on the two assumptions.

First, it is assumed that the inverse heat conduction problem to be linear, i.e., $\theta_{\mathrm{ps}} = \sum_{j=1}^{M} P^j q_s^j$, where the vector P^j is the surface temperature response to a unit step heat flux at time j, q_s^j is the heat flux magnitude at time j. Another assumption is that the effect of heat flux at time j on the surface temperature change is instantaneous. If the history of surface temperature response to the unite step heat flux is $(T^1, T^2, \cdots T^M)^T$, then $P^j = (0, \cdots, 0, T^j, 0, \cdots, 0)^T$ ($j = 1, 2, \cdots, M$) and a diagonal matrix Φ' has the nonzero elements $(T^1, T^2, \cdots, T^M)$ only in the diagonal line.

To obtain Φ', a unit step heat flux is applied to the system of equations and the surface temperature is determined by using the numerical method for the direct problem for a step function of heat flux. From the initial condition for the polymer, we know $T^1 = 0$, and hence the first row and first column of Φ' are zero vectors. The first row and first column of Φ' are therefore discarded. Because of discarding the data, the first heat flux estimate q_s^1 cannot be determined. Fortunately, we can set q_s^1 to be zero in most time. For the nonsingular matrix Φ'_{2-M}, the history of heat flux can be estimated by $q_s^{2-M} = \Phi'^{-1}_{2-M}\theta_{\mathrm{ps}}^{2-M}$. Since Φ'_{2-M} is a diagonal matrix, it is easy to compute the inverse matrix. The initial (coarse) determination of heat flux is simple and fast. For some simple simulated histories of heat flux, the recovered results are good enough as the initial approximation for the subsequent optimization. Hereafter, we use Φ to denote the nonsingular matrix Φ'_{2-M} by neglecting the influence of the initial condition.

B. Optimization

The determination of heat flux can be mathematically described as the following optimization problem:

$$\min_{q_s} \|\theta_{\mathrm{ps}} - \theta'_{\mathrm{ps}}(q_s)\|_2^2 \tag{7}$$

where q_s is the heat flux to be found, and θ'_{ps} is the estimated surface temperature response to q_s that is calculated by solving the system of equations for the positive problem. The difference between the estimated temperature and TSP-measured temperature is minimized, and an iterative algorithm to solve the optimization problem is described in Table 1. The error bound ε in calculations of heat flux from TSP data is set at 10^{-5}.

IV. Simulations

A. Constant Thermal Properties

To examine the algorithm, we consider a polyvinyl chloride (PVC) layer on a semi-infinite aluminum base and a Nylon-6 base. The initial step change followed by a sinusoidal change in heat flux is used to simulate the transient starting process in the Boeing/AFOSR Mach-6 Quiet Tunnel at Purdue University, as shown in Fig. 2. The time histories of temperature on a 0.01 mm thick PVC surface on a semi-infinite aluminum base and a Nylon-6 base are generated by solving the system of equations. Figure 3 shows the resulting temperature histories responding to the simulated heat flux change, where T_{surface} and $T_{\mathrm{interface}}$ are the temperatures at the polymer surface ($y = L$) and interface between the polymer and base ($y = 0$), respectively. A comparison is made between the numerical and analytical inverse methods. As indicated in Fig. 4, the numerical and analytical inverse methods are in good agreement for the constant thermal properties, and the numerical algorithm gives satisfactory recovery of heat flux after five iterations. For a PVC layer on a

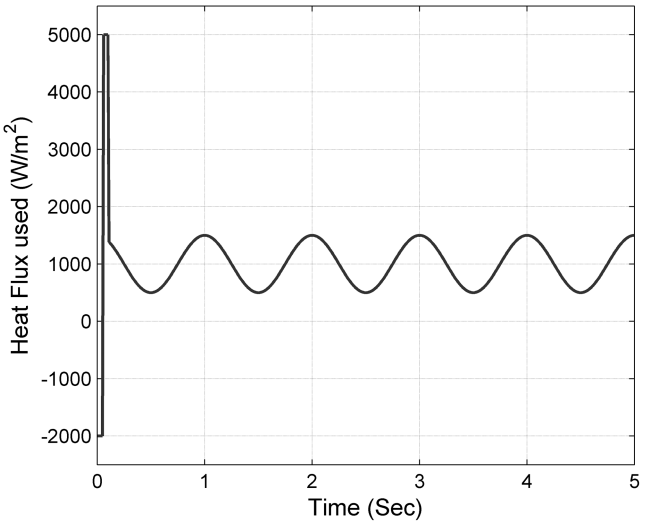

Fig. 2 The simulated heat flux with starting step changes followed by a sinusoidal change.

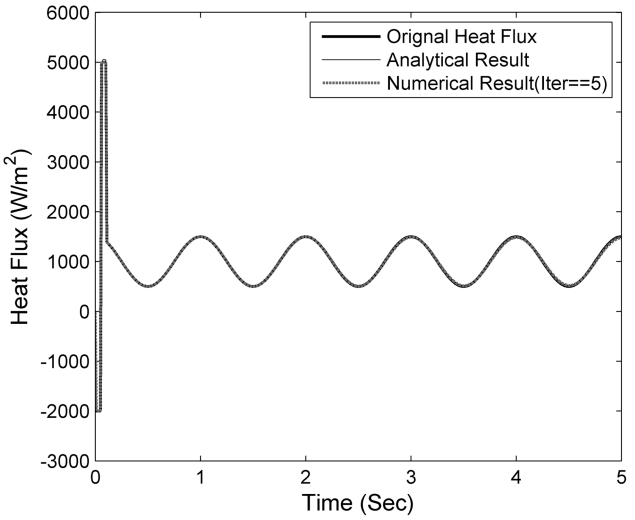

Fig. 4 Comparison of the recovered heat flux by using the inverse numerical method and analytical inverse method for a 0.01 mm PVC layer on a semi-infinite aluminum base.

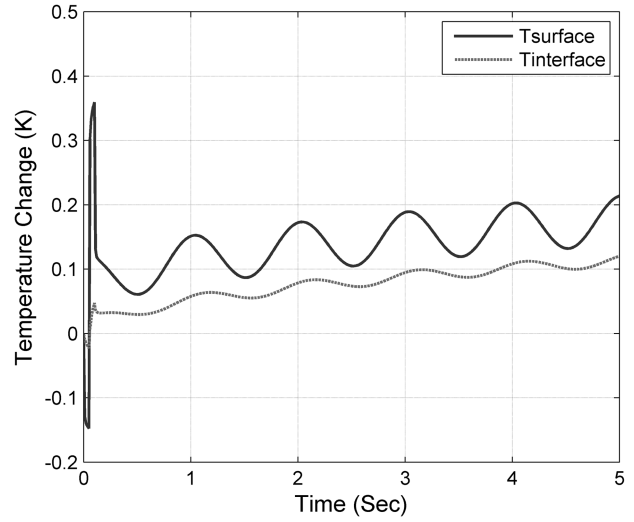

a)

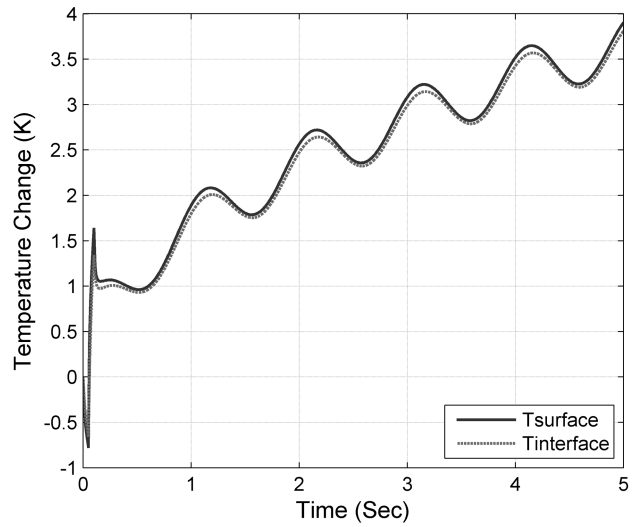

b)

Fig. 3 The temperature history at the surface and interface between the 0.01 mm thick PVC sheet and a semi-infinite base responding to the simulated heat flux: a) aluminum and b) Nylon-6 base.

semi-infinite Nylon-6 base is also considered, the iterative algorithm converges to the original heat flux history after 20 iterations.

B. Temperature-Dependent Thermal Properties

The analytical inverse method is based on an assumption that the thermal properties of the polymer and base layers are constant. This assumption is reasonably good for many applications. However, when the surface temperature change is sufficiently large in hypersonic testing, the effects of the temperature dependencies of the thermal properties should be considered for more accurate determination of heat flux. The thermal properties may change with increasing the surface temperature during a run. To take the temperature dependencies of the thermal properties into account, the coefficient matrix in the linear system of equations is updated after each time step, depending on the thermal properties that are given as the specified functions of temperature.

To illustrate the effects of temperature dependencies of the thermal properties, we consider the simulated heat flux with a starting step change followed by a sinusoidal change into a 0.01 mm PVC layer covered on an aluminum base and a Nylon-6 base. According to the data provided by Bryce [17], the specific heat and thermal conductivity of PVC are fitted by the empirical formula $c(T) = 1540 + 4(T - 293)$ and $k(T) = 0.16 - 0.0004(T - 293)$, respectively, where T is temperature in Kelvin, c is in J/kg-K, and k is in W/m-K. It is assumed that the density of PVC is independent of temperature, i.e., $\rho = 1300$ kg/m^3. Therefore, the thermal diffusivity of PVC is

$$a(T) = \frac{k}{c\rho} = \frac{0.16 - 0.0004(T - 293)}{[1540 + 4(T - 293)] \cdot 1300} \tag{8}$$

For simplicity, it is assumed that the thermal properties of the base (aluminum or Nylon-6) are constant, as shown in Table 2.

In principle, the numerical inverse method can recover heat flux by taking the temperature dependencies of the thermal properties into account. The simulated heat flux history shown in Fig. 2 is used again. Based on the surface temperature history simulated by using

Table 2 Thermal properties of polymer and base materials

Properties	PVC (293 K)	Stainless steel	Al	Nylon-6
k (W/m-K)	0.16	16	204	0.25
ρ (kg/m^3)	1300	7900	2700	1140
c (J/kg-K)	1540	500	904	1670

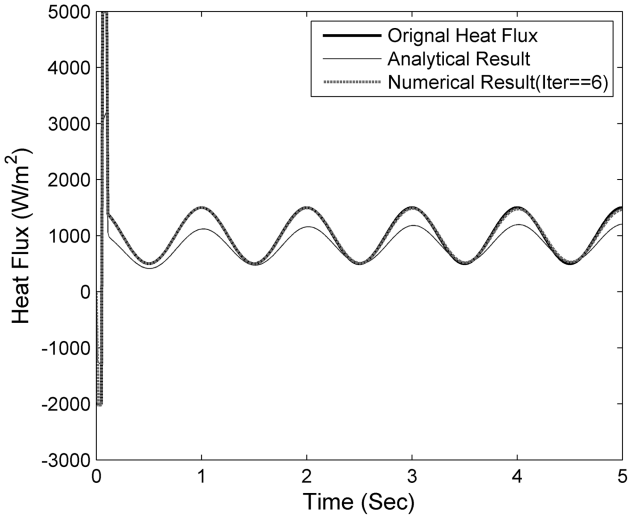

Fig. 5 Comparison of the recovered heat flux by using the numerical inverse method and analytical method for a 0.01 mm PVC layer on a semi-infinite aluminum base, where the thermal properties of PVC are temperature-dependent.

the temperature-dependent thermal properties, heat flux is calculated by using the numerical inverse method, and good convergence to the original heat flux is achieved after six iterations for a 0.01 mm PVC layer on a semi-infinite aluminum base. Figure 5 shows a comparison with the analytical inverse method that is valid only for the constant thermal properties. As expected, in this case, the numerical inverse method can recover the correct heat flux history, while the analytical inverse method has a considerable error.

The simulated surface temperature for a PVC layer on a semi-infinite Nylon-6 base is also considered. A comparison of the recovered results between the numerical inverse method and the analytical inverse method is shown in Fig. 6. In this case, the analytical inverse method still can achieve as good recovery of heat flux as the numerical inverse method. Interestingly, the temperature dependencies of the thermal properties do not significantly affect on the calculation of the surface heat flux in the case of a low-conductive base. The insensitivity of heat flux calculation on the thermal properties for a low-conductive base like Nylon-6 has been found in an error analysis given by Liu et al. [15].

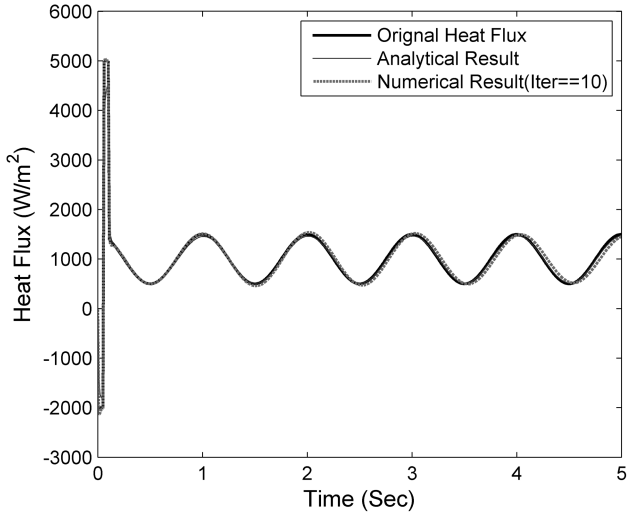

Fig. 6 Comparison of the recovered heat flux by using the numerical inverse method and analytical method for a 0.01 mm PVC layer on a semi-infinite Nylon-6 base, where the thermal properties of PVC are temperature-dependent.

V. Experiments

A. 48-Inch Shock Tunnel

To examine the accuracy of the numerical inverse method, raw TSP images on the sharp 25°/45° indented cone model are reprocessed, which were obtained by Hubner et al. [2] in run number 46 at Mach 11 in the 48 in. Shock Tunnel at Calspan University of Buffalo Research Center. The detailed descriptions of the experimental setup and procedures are given by Hubner et al. [2]. The model was made of stainless steel. Over 60 platinum thin-film heat transfer gauges were installed along a ray of the model, providing heat flux data for comparison with TSP. The reported measurement accuracy of the gauges is ±5%, and the measurement resolution is 5 kW/m^2. TSP was Ru-phen in a nonoxygen-permeable polyurethane binder. The TSP calibration data are fit by a polynomial:

$$T/T_{\text{ref}} = \sum_{n=0}^{8} a_n [\ln(I_{\text{ref}}/I)]^n \tag{9}$$

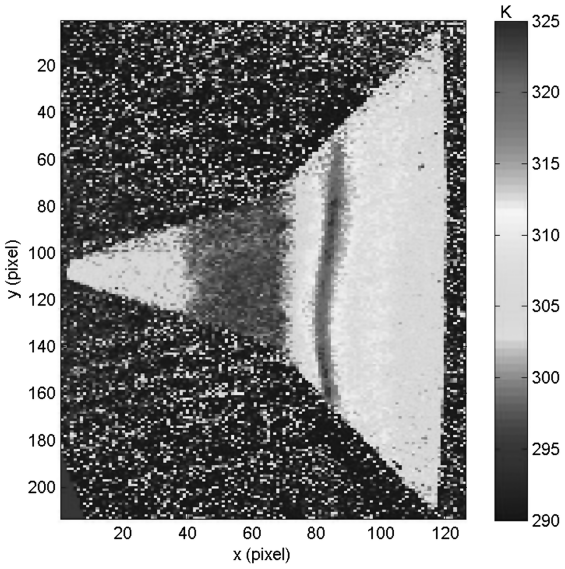

a)

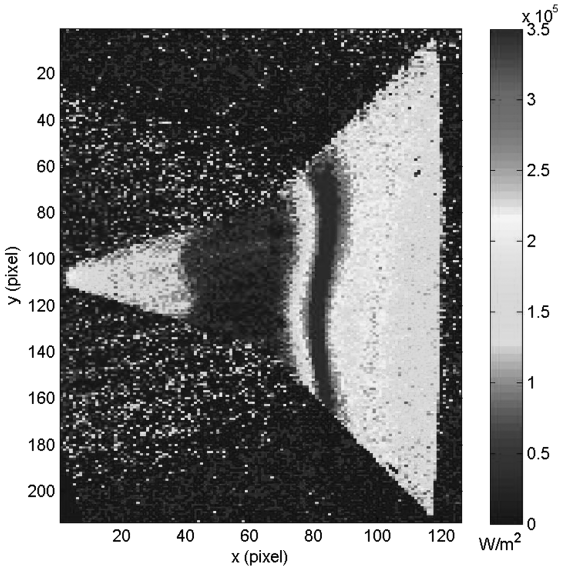

b)

Fig. 7 Surface temperature and heat flux: a) temperature image and b) averaged heat flux image of the sharp 25°/45° indented cone model at Mach 11 (the original TSP images from Hubner et al. [2]).

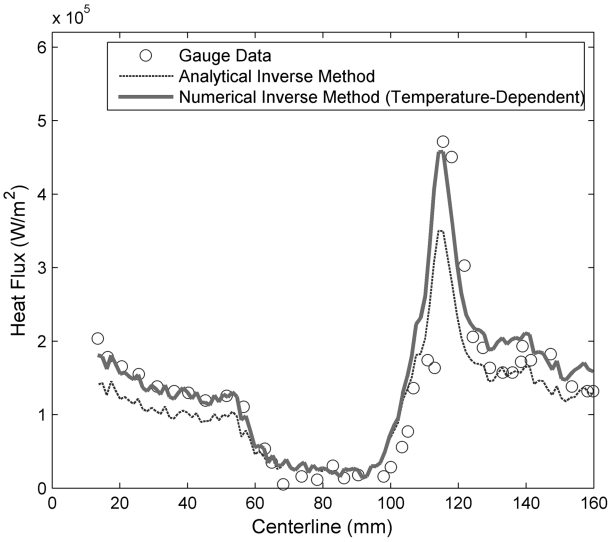

Fig. 8 The averaged heat distributions along the centerline on the sharp 25°/45° indented cone model at Mach 11.

where $a_0 = 1.0$, $a_1 = 0.1167$, $a_2 = 0.0853$, $a_3 = -0.1404$, $a_4 = -0.2186$, $a_5 = 0.498$, $a_6 = -0.3386$, $a_7 = 0.0996$, and $a_8 = -0.0109$. The reference temperature T_{ref} in Eq. (9) was 295 K. The thickness of TSP was 10 μm, and the white polyurethane base coat was 40 μm. Thus, the total thickness of the polymer layer was 50 μm. In image processing, the raw flow-off and flow-on TSP images are corrected by subtracting the background intensity that is contributed by the ambient light and leakage of the optical filter before taking a ratio between the flow-off and flow-on images. Then, the ratio images are converted to the temperature images by using a priori calibration data.

The analytical inverse method has been used previously to obtain the heat flux distributions for this case without considering the temperature dependencies of the thermal properties of the materials [15]. Here, it is assumed in the numerical inverse heat flux calculation that the polymer layer (TSP plus the base coating) has the same temperature dependencies as PVC in the thermal properties, which are described in Sec. IV.B. The thermal properties of the stainless steel base are assumed to be constant. Figure 7 shows a typical surface temperature image selected from a total of 16 temperature images in the run and the averaged heat flux image in an interval of 4–6 ms in which the flow was stabilized. The heat flux distributions along the centerline are shown in Fig. 8, where the numerical inverse method incorporates the temperature dependencies of the thermal properties in contrast to the analytical inverse method. The numerical inverse method gives the improved result that is closer to the data given by an array of thin-film heat flux gauges. The effect of the temperature dependencies of the thermal properties is pronounced in this case because the increase of the polymer temperature on the metal base is relatively large (about 20 K) in this tunnel.

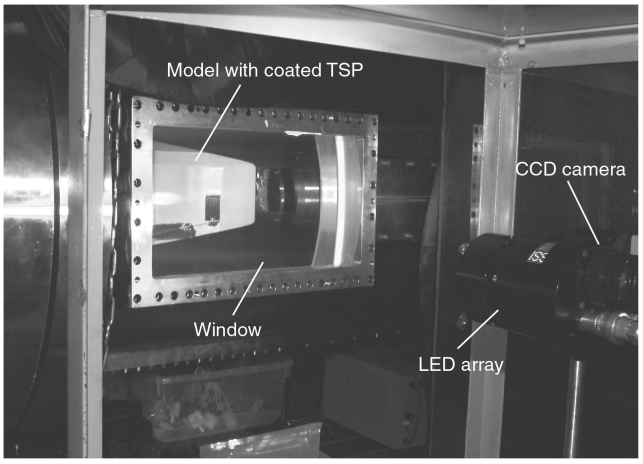

Fig. 9 A generic setup of a CCD camera and a UV LED array for illuminating the TSP on a model at the Purdue Mach-6 tunnel.

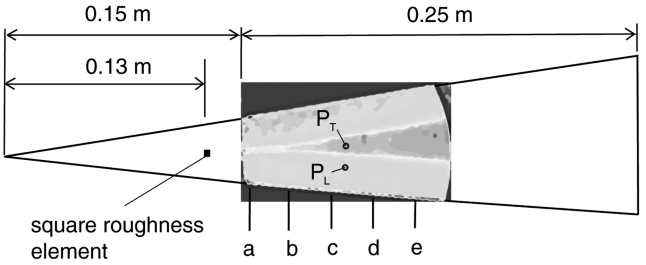

Fig. 10 Region of TSP measurements on a 7°-half-angle circular cone.

B. Boeing/AFOSR Mach-6 Quiet Tunnel

TSP measurements on a 7° half-angle Nylon-6 cone were conducted at zero angle of attack in the Boeing/AFOSR Mach-6 Quiet Tunnel at Purdue University [24,25]. The stagnation temperature and pressure were 433 K and 255 psi, respectively. The 7°-half-angle nylon cone is 0.4 m (16 in.) long, including a 0.15 m long stainless steel nose tip that has a 1.52 mm (0.06 in.) nose radius. The TSP, Ru (bpy) in Chromaclear auto paint, was directly coated on the nylon surface. The coating thickness was about 50 microns. The temperature calibration for this TSP is given by [25]

$$T/T_{\text{ref}} = \sum_{n=0}^{4} C_n (I/I_{\text{ref}})^n \tag{10}$$

where $C_0 = 1.2342$, $C_1 = -0.3804$, $C_2 = 0.3443$, $C_3 = -0.2543$, and $C_4 = 0.0542$ in a range of $0.9 < T/T_{\text{ref}} < 1.1$. For temperature conversion from the luminescent intensity of TSP in this test, the reference temperature in Eq. (10) is $T_{\text{ref}} = 298$ K.

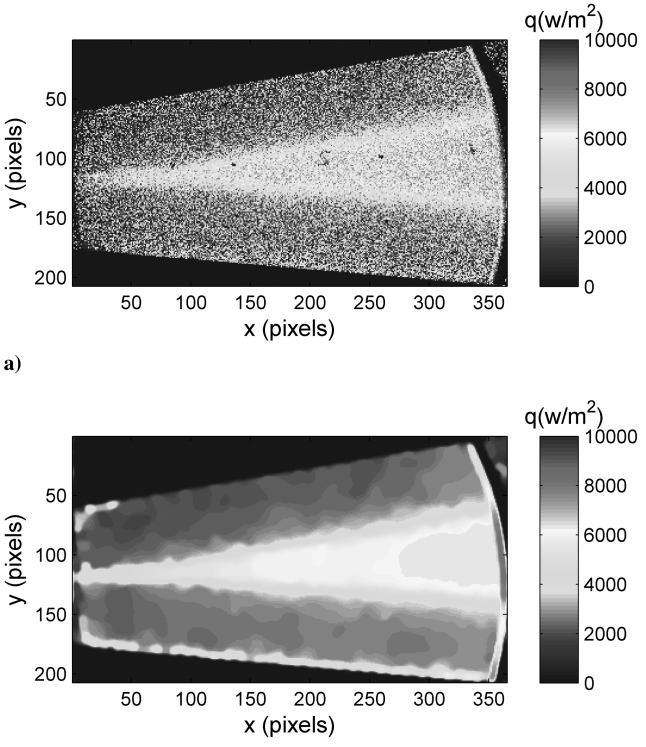

Fig. 11 Heat flux images on a 7°-half-angle circular cone at Mach 6 at $t = 3$ s: a) image obtained by using the numerical inverse method and b) image improved by using the image deconvolution method.

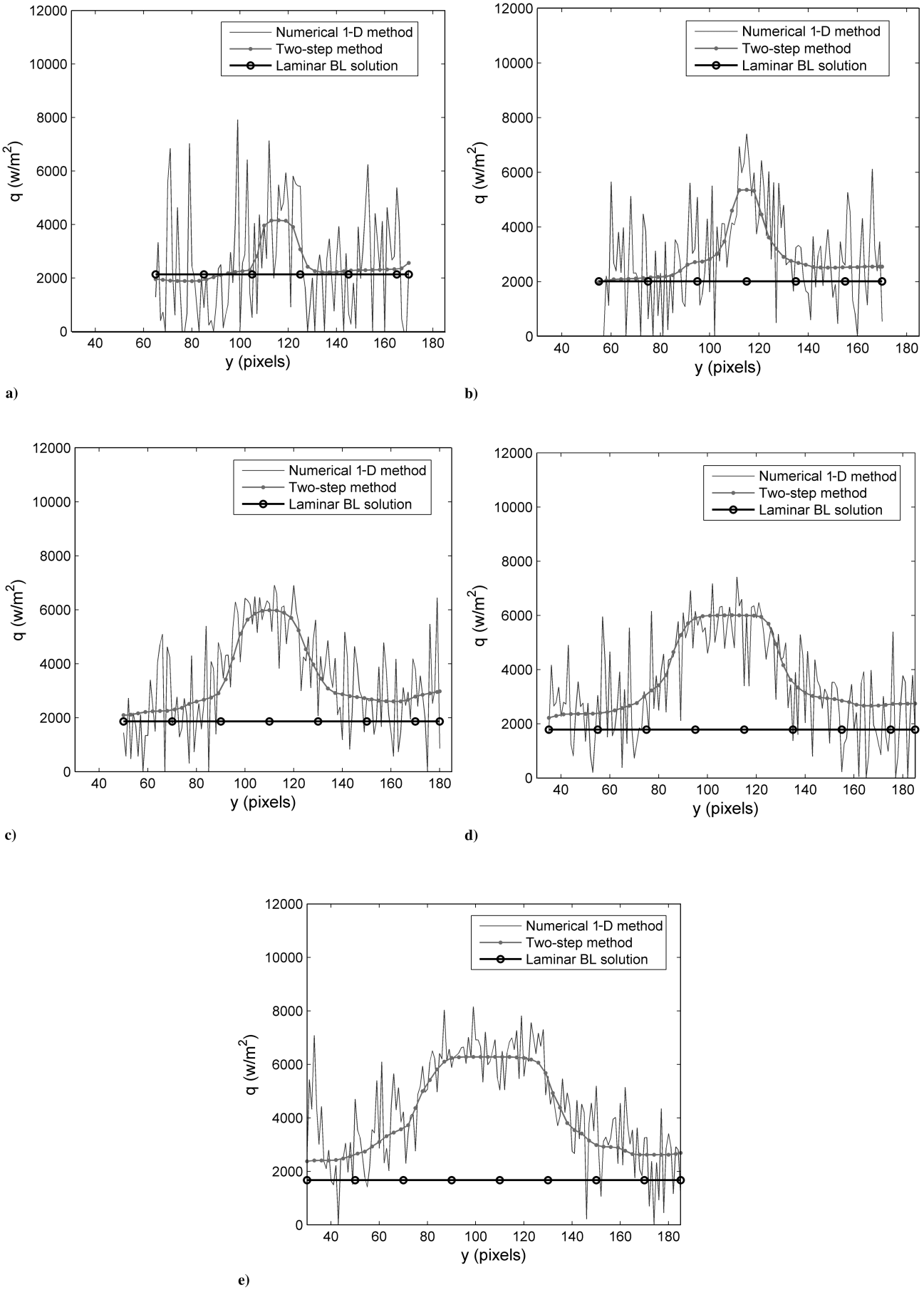

Fig. 12 Heat flux distributions across the cone at a) $x = 0.16$ m, b) 0.18 m, c) 0.21 m, d) 0.23 m, and e) 0.26 m at $t = 3$ s from starting the tunnel. The results are obtained by the numerical inverse method with the temperature-dependent thermal properties in comparison with the laminar boundary-layer solution. Further, the results are improved by using the image deconvolution method.

Figure 9 shows a generic setup of a charge-coupled device (CCD) camera with a band-pass optical filter for detecting the luminescent emission from the TSP and a blue light-emitting diode (LED) array (460 nm) for illuminating the TSP on a model in a dark environment in the Mach-6 tunnel. The camera (PCO 1600) and blue LED array are purchased from Innovative Scientific Solutions, Inc.** The time step in a sequence of 45 images acquired by the camera was 0.107 s. In our experiments where the total pressure was relatively high, a smaller circular window was used. A viewed region near the middle section of the cone is illustrated in Fig. 10. A square roughness element with a 1.27×1.27 mm^2 cross section and a height of 0.28 mm was placed at 0.13 m from the nose tip to trigger the boundary-layer transition to turbulence. The basic testing procedures of TSP in wind tunnels are described by Liu and Sullivan [26].

Surface temperature images were obtained by using Eq. (10) from a sequence of TSP images, and then heat flux images are calculated at every pixel by using the numerical inverse method and analytical inverse method. It is again assumed that the TSP has the same thermal properties as PVC described in Sec. IV.B. Table 2 lists the thermal properties of PVC and Nylon-6. Figure 11a shows a heat flux image obtained by using the one-dimensional numerical inverse method on a 7°-half-angle circular cone at Mach 6 at $t = 3$ s from starting the tunnel. In this case, the effect of the temperature dependencies of the thermal properties of the polymer is negligible for a small change of temperature on the Nylon-6 base (see the simulation in Sec. IV.B). The significant spike noise found in these images is typical in TSP measurements particularly when the measured temperature change is small (less than a few degrees). Figure 11b shows the corresponding heat flux image improved by applying the image deconvolution method to Fig. 11a to correct the lateral heat conduction effect and remove the random noise [16]. These images clearly indicate the formation and development of a turbulent wedge triggered by a roughness element in the boundary layer, which is evidenced by the difference in heat flux between the turbulent and laminar flow regimes.

Figure 12 shows the heat flux distributions in the vertical direction in images across the cone at the streamwise locations $x = 0.16$, 0.18, 0.21, 0.23 and 0.26 m at $t = 3$ s from starting the tunnel along with the local values of heat flux given by the laminar boundary-layer solution. For illustration, these locations are marked in Fig. 10. In fact, these distributions are the projected ones of those on a circular arc of a local cross section of the cone. Then, the improved distributions of heat flux are obtained by applying the image deconvolution method to correct the lateral heat conduction effect and reduce the random spike noise [16]. This approach is called the two-step method (the one-dimensional inverse method coupled with the image deconvolution method). This improvement is particularly appealing for the result at $x = 0.16$ m where the random noise is very large relative to the signal. At $x = 0.16$ and 0.18 m where the turbulent wedge is narrow in its width and weak in its magnitude of heat flux, the TSP-measured values of heat flux outside of the wedge are consistent with the prediction by the laminar boundary-layer solution on the cone. However, when the turbulent wedge considerably diffuses (expands) in the lateral direction as it develops downstream, the TSP-measured value of heat flux outside of the turbulent wedge deviates gradually from the prediction by the laminar boundary-layer solution. This deviation is more evident at $x = 0.23$ and 0.26 m, indicating that there is increasing influence of the turbulent wedge diffused along the lateral direction.

VI. Conclusions

The numerical inverse method is developed to determine heat flux from TSP images obtained in short-duration hypersonic tunnels. This method is an iterative algorithm based on a numerical solution for the positive heat transfer problem and an optimization scheme to minimize the error between the calculated and measured surface temperatures. Simulations indicate that the numerical and analytical inverse methods give the same result of heat flux for a simulated tunnel run when the thermal properties of the TSP and base materials are constant. Nevertheless, the numerical inverse method has the major advantage that it can take the effect of the temperature dependencies of the thermal properties into account in computations. The numerical inverse method is applied to TSP measurements on a sharp stainless steel 25°/45° indented model at Mach 10 and a sharp 7°-half-angle Nylon-6 cone model with a roughness element at Mach 6. The extracted heat flux distributions are compared favorably with those given by thin-film heat transfer gauges and the laminar boundary-layer solution.

**http://www.innssi.com [retrieved 15 Oct. 2009].

Acknowledgments

This work is supported by NASA Research Announcement grant NNX08AC97A. We would like to thank Steven Schneider and his group for collaborations in measurements in the Boeing/AFOSR Mach-6 Quiet Tunnel at Purdue University.

References

[1] Liu, T., Campbell, B., Sullivan, J., Lafferty, J., and Yanta, W., "Heat Transfer Measurement on a Waverider at Mach 10 Using Fluorescent Paint," *Journal of Thermophysics and Heat Transfer*, Vol. 9, No. 4, 1995, pp. 605–611. doi:10.2514/3.714

[2] Hubner, J. P., Carroll, B. F., and Schanze, K. S., "Heat-Transfer Measurements in Hypersonic Flow Using Luminescent Coating Techniques," *Journal of Thermophysics and Heat Transfer*, Vol. 16, No. 4, 2002, pp. 516–522. doi:10.2514/2.6726

[3] Norris, J. D., Hamner, M., Lafferty, J. F., Smith, N. T., and Lewis, M. J., "Adapting Temperature-Sensitive Paint Technology for Use in AEDC Hypervelocity Wind Tunnel 9," AIAA Paper 2004-2191, 2004.

[4] Kurits, I., Lewis, M., Hamner, M., and Norris, J. D., "Development of a Global Heat Transfer Measurement System at AEDC Hypervelocity Wind Tunnel 9," 22nd International Congress on Instrumentation in Aerospace Simulation Facilities, Pacific Grove, CA, 2007.

[5] Matsumura, S., Berry, S. A., and Schneider, S. P., "Flow Visualization Measurement Techniques for High-Speed Transition Research in the Boeing/AFOSR Mach-6 Quiet Tunnel," AIAA Paper 2003-4583, July 2003.

[6] Matsumura, S., Schneider, S. P., and Berry, S. A., "Streamwise Vortex Instability and Transition on the Hyper-2000 Scramjet Forebody," *Journal of Spacecraft and Rockets*, Vol. 42, No. 1, 2005, pp. 78–88. doi:10.2514/1.3959

[7] Schneider, S. P., Rufer, S., Skoch, C., and Swanson, E., "Hypersonic Transition Research in the Boeing/AFOSR Mach-6 Quiet Tunnel," AIAA Paper 2003-3450, June 2003.

[8] Schultz D. L, and Jones, T. V., "Heat Transfer Measurements in Short-Duration Hypersonic Facilities," AGARD Rept. No. 165, 1973.

[9] Cook, W. J., and Felderman, E. J., "Reduction of Data from Thin-Film Heat Transfer Gages: A Concise Technique," *AIAA Journal*, Vol. 8, No. 7, 1970, pp. 1366–1368. doi:10.2514/3.5909

[10] Merski, N. R., "Reduction and Analysis of Phosphor Thermography Data with the IHEAT Software Package," AIAA Paper 98-0712, 1998.

[11] Merski, N. R., "Global Aeroheating Wind-Tunnel Measurements Using Improved Two-Color Phospher Thermography Method," *Journal of Spacecraft and Rockets*, Vol. 36, No. 2, 1999, pp. 160–170. doi:10.2514/2.3446

[12] Walker, D. G., and Scott, E. P., "Evaluation of Estimation Methods for High Unsteady Heat Fluxes from Surface Measurements," *Journal of Thermophysics and Heat Transfer*, Vol. 12, No. 4, 1998, pp. 543–551. doi:10.2514/2.6374

[13] Lin, M., and Wang, T., "A Transient Liquid Crystal Method Using a 3-D Inverse Transient Conduction Scheme," *International Journal of Heat and Mass Transfer*, Vol. 45, No. 17, 2002, pp. 3491–3501. doi:10.1016/S0017-9310(02)00073-X

[14] Wang, T., Lin, M., and Bunker, R. S., "Flow and Heat Transfer of Confined Impingement Jets Cooling Using 3-D Transient Liquid Crystal Scheme," *International Journal of Heat and Mass Transfer*, Vol. 48, Nos. 23–24, 2005, pp. 4887–4903. doi:10.1016/j.ijheatmasstransfer.2005.04.020

[15] Liu, T., Cai, Z., Lai, J., Rubal, J., and Sullivan, J., "Analytical Methods for Determining Heat Flux from Temperature-Sensitive-Paint Measurements in Hypersonic Tunnels," *Journal of Thermophysics and Heat Transfer*, Vol. 24, No. 1, 2010, pp. 85–94.

doi:10.2514/1.43372
[16] Liu, T., Wang, B., Rubal, J., and Sullivan, J., "Correcting Lateral Heat Conduction Effect in Image-Based Heat Flux Measurements as an Inverse Problem," *International Journal of Heat and Mass Transfer* (to be published).
doi:10.1016
[17] Bryce, D. M., *Troubleshooting: A Guide for Injection Molders*, Techtrax, Georgetown, D.C., 2001, Chap. 2.
[18] Morton, K. W., and Mayers, D. F., *Numerical Solution of Partial Differential Equations: An Introduction*, Cambridge Univ. Press, Cambridge, England, U.K., 1994.
[19] Fletcher C. A. J., *Computational Techniques for Fluid Dynamics*, Springer, Berlin, 1988.
[20] Hoffman, J. D., *Numerical Methods for Engineers and Scientists*, McGraw–Hill, New York, 1992.
[21] Stolz, G. J., "Numerical Solutions to an Inverse Problem of Heat Conduction for Simple Shapes," *Journal of Heat Transfer*, Vol. 82, Feb. 1960, pp. 20–26.
[22] Beck J. V, Blackwell, B., and Clair, C. S., *Inverse Heat Conduction: Ill-Posed Problems*, Wiley, New York, 1985.
[23] Alifanov, O. M., *Inverse Heat Transfer Problems*, Springer, Berlin, 1994.
[24] Casper, K. M., Wheaton, B. M., Johnson, H. B., and Schneider, S. P., "Effects of Freestream Noise on Roughness-Induced Transition at Mach 6," AIAA Paper 2008-4291, 2008.
[25] Swanson, E. O., "Boundary Layer Transition on Cones at Angle of Attack in a Mach-6 Quiet Tunnel," Ph.D. Thesis, School of Aeronautics and Astronautics, Purdue Univ., 2008.
[26] Liu, T., and Sullivan, J., *Pressure and Temperature Sensitive Paints*, Springer, Berlin, 2004, Chap. 10.